Performance Requirements of Membrane Reactors for the Application in Renewable Methanol Synthesis: A Techno-Economic Assessment

Vincent Dieterich,* Nicolas Wein, Hartmut Spliethoff, and Sebastian Fendt*

Renewable energy carriers are expected to play a key role in the defossilization of the energy and chemical sector. For renewable methanol synthesis, membrane reactors (MR) have been tested on a laboratory-scale with promising results. However, membrane performance requirements that allow an economic benefit for their large-scale deployment are missing. Therefore, a 1D Python MR model is coupled with an AspenPlus process simulation to conduct a techno-economic assessment with focus on membrane performance. Two synthesis loop configurations are investigated: one where feed and sweep recycle are operated at the same pressure and one where the sweep recycle operates at atmospheric pressure. The results show that both configurations can offer technical benefits, if sufficiently high product separation can be achieved, but that for a compressed sweep recycle no economic benefits are possible. As a consequence, membranes used for methanol synthesis must endure operation at high pressure differences. Furthermore, the results highlight the critical role of the H_2 permeance, which should remain below 1×10^{-9} mol m^{-2} s^{-1} Pa^{-1}. From an economic standpoint high water permeation has a more beneficial effect than high methanol permeation.

1. Introduction

For the transformation of the energy system away from fossil fuels, renewable energy carriers are seen as an essential part of the solution. Applications range from defossilization of the mobility sector (e.g., aviation or shipping) to the provision of sustainable chemicals. A variety of potential chemicals have been discussed as renewable energy carriers, for example, methane, methanol, dimethyl ether, Fischer–Tropsch fuels, or ammonia. While their properties vary, their synthesis share some characteristics namely that they are formed in exo-

thermic reactions with a limitation of the conversion due to the chemical equilibrium.[1] As a consequence, large scale production usually requires the recycling of unconverted reactant gases, which results in larger unit operations and increased operational costs. One approach to improve conversion and reduce the recycling effort is the in situ product removal in the reactor to avoid the equilibrium limitations. This has the potential to increase the overall energy efficiency and thereby reducing the costs of renewable energy carriers.

Membrane technologies for product separation have been investigated for years now and are already used on an industrial scale for some applications.[2] Membrane reactors (MR), however, have not been applied industrially for thermochemical syntheses, for example, methanol synthesis. While current research has shown the potential of membrane reactors for the synthesis of renewable energy carriers and allowed the proof-of-concept, it usually focuses on specific membrane types for experimental research or investigates the concept on a broader techno-economic level with specific assumptions for the membrane performance. Benchmarks for membrane development allowing to move beyond laboratory scale are missing, however.

This article wants to close this gap and derive important performance targets for the membrane to enable benefits on the overall process level and the process economics. The goal is to provide researchers working on material improvements with targets to aim for and process engineers and industry experts with guidelines in which cases the industrial application of MRs might be beneficial.

For this purpose renewable methanol synthesis from H_2 and CO_2 has been selected as a case study. Methanol is one of the most discussed potential renewable energy carriers due to its wide application even today and the potential to use methanol as fuel in conventional engines and fuel cells. **Figure 1** shows the general approach taken in this work. An elaborate process model for the methanol synthesis with a MR has been developed by coupling the flowsheet simulation tool Aspen Plus with a Python MR model. Two cases have been investigated. First, a case where sweep and feed pressure are equal and no pressure difference exists between retentate and permeate side. Second,

V. Dieterich, N. Wein, H. Spliethoff, S. Fendt
Chair of Energy Systems
Technical University of Munich
Boltzmannstr. 15 85748, Garching, Germany
E-mail: vincent.dieterich@tum.de; sebastian.fendt@tum.de

**ADVANCED
SCIENCE NEWS**

www.advancedsciencenews.com

**ADVANCED
SUSTAINABLE
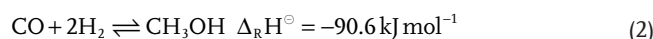SYSTEMS**

www.advsustainsys.com
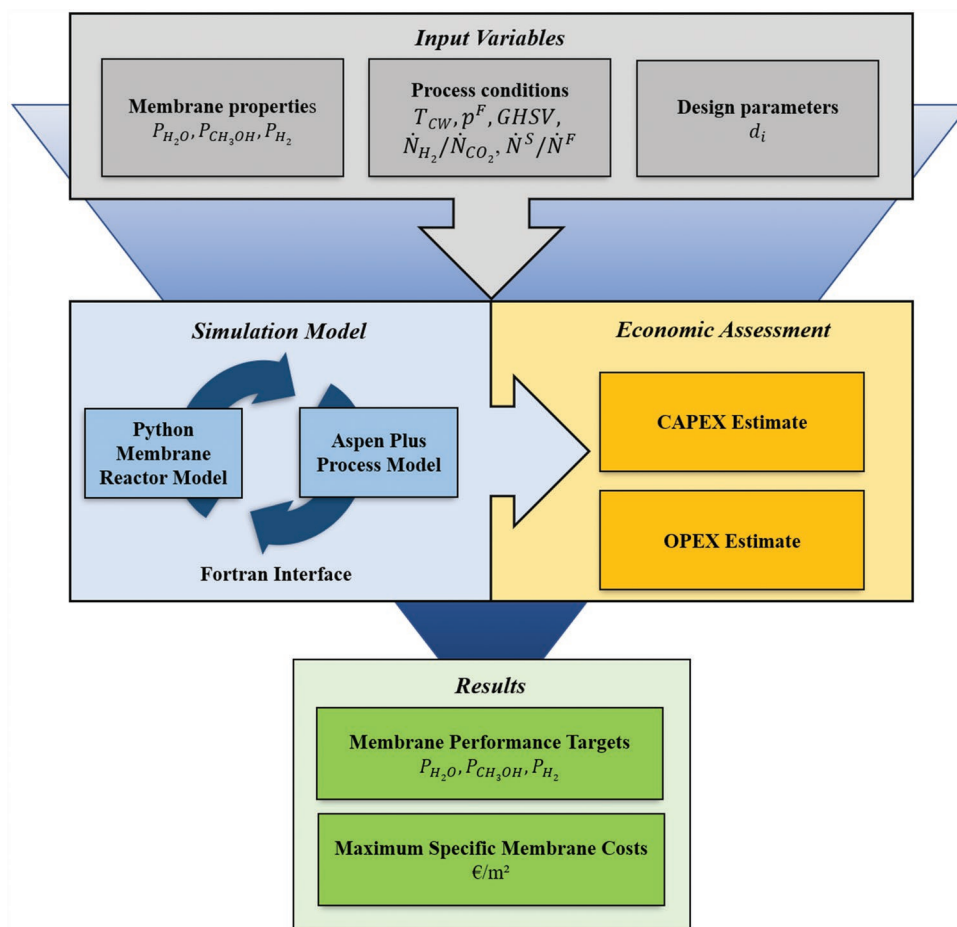
Figure 1. Approach taken in this work to determine performance as well as cost targets for membranes used for methanol synthesis.

a case with atmospheric sweep recycle. The simulation results are then used in an economic assessment and performance as well as cost targets for the membrane are determined.

Based on conducted parameter studies it can be confirmed that MRs might benefit the overall process performance and economics of renewable methanol synthesis. However, the results suggest that they are not necessarily the better option economically, instead it depends highly on the process conditions and the achievable membrane performances. This is due to the necessity of an additional sweep recycle that limits the economic benefits of the membrane process compared to the conventional synthesis.1.1. Methanol Synthesis

Conventional industrial methanol synthesis has been investigated for more than a century.[3] Usually, the synthesis gas feed (mainly CO and H_2) is generated from natural gas or coal and converted via an exothermic, heterogeneous catalyzed reaction to methanol. For renewable methanol via biomass-to-X or power-to-X, direct conversion of CO_2 with H_2 is an option and is considered exclusively in this work. A detailed description of the synthesis process including catalysis, reactor design and product purification has been given in a recent review by the authors.[4] Industrial low pressure synthesis of methanol is operated between 200 and 300 °C, determined by the activity of the applied copper catalysts and limited by the catalysts thermal

stability. Methanol is formed in two equilibrium reactions given in Equations (1) and (2).

$$CO_2 + 3H_2 \rightleftharpoons CH_3OH + H_2O \quad \Delta_R H^{\ominus} = -49.4 \, kJ \, mol^{-1} \qquad (1)$$

$$CO + 2H_2 \rightleftharpoons CH_3OH \quad \Delta_R H^{\ominus} = -90.6 \, kJ \, mol^{-1} \qquad (2)$$

In addition, since CO_2 and H_2 are present the reverse water gas shift reaction (rWGS) in Equation 3 has to be taken into account.

$$CO_2 + H_2 \rightleftharpoons CO + H_2O \quad \Delta_R H^{\ominus} = 41.2 \, kJ \, mol^{-1} \qquad (3)$$
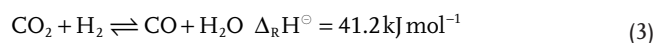
Both synthesis reactions are exothermic and involve a volume reduction. Thus, according to Le Chatelier's principle the synthesis of methanol is favored by low temperatures and high pressures. Even though methanol production is a mature process, the maximum per-pass conversion is still a challenge due to the chemical equilibrium. It is theoretically limited to around 25%, whereas only 4–14% are achieved under real conditions.[3] To overcome the conversion limitation, high recycle rates are necessary. In order to achieve an almost complete carbon conversion rate (typically 93–98%), the recycle to process feed gas ratio must reach values between 3 to 5.[4] However,

**ADVANCED
SCIENCE NEWS**

www.advancedsciencenews.com

**ADVANCED
SUSTAINABLE
SYSTEMS**

www.advsustainsys.com

high recycle ratios go along with larger unit operations, that is, larger reactor, compressors and separators, hence resulting in higher investment costs.

1.2. Current Research on Membrane Reactors for Methanol Synthesis

MRs for methanol synthesis have been considered for more than a decade. For example, Struis et al. proved that MRs can improve the reactant conversion and methanol yield in their experiments in the 1990s.[5] In general, polymer, carbon, and zeolite membranes have been considered for methanol synthesis.[6] However, polymeric membranes have not been investigated further because of their low temperature stability and carbon membranes are still in early development. Consequently, inorganic zeolite membranes are seen as the most promising option for methanol synthesis reactors.[7]

Membranes and MR concepts for methanol synthesis have been investigated experimentally as well as simulatively. Gallucci et al. investigated an A-type zeolite MR to increase CO_2 conversion. They reported an increase from 2.7% to 8.7% for the single pass conversion of CO_2. A similar investigation has been conducted by Gorbe et al. who saw promising water separation factors up to 240 °C.[8] Sawamura et al. evaluated the water-methanol-hydrogen separation properties of a mordenite membrane at temperatures as high as 250 °C.[9] Li et al. recently investigated zeolite membranes made of water-conducting nanochannels that allow highly selective water removal within the reactor.[10] Their results show an increase of the methanol yield to 39.8% compared to 14% in the conventional reactor.

Table 1 gives a short overview of currently achievable permeances for zeolite membranes in literature. Highest water permeance is around 1×10^{-6} mol m^2 s^{-1} Pa^{-1}), while highest methanol permeance is an order of magnitude lower between 1×10^{-7}–210^{-7} mol m^2 s^{-1} Pa^{-1}.

The experimental results have been confirmed by simulative studies that agree in the potential of MRs to improve conversion and methanol yield.[14,15] Atsonius et al. compared the effects of pure in situ water removal and pure methanol removal in the MR by using a cascade of equilibrium reactor models and separator models to mimic the membrane separation.[16] In both cases significant improvements in the methanol yield were observed while their techno-economic assessment indicated that due to the high hydrogen costs the renewable synthesis of methanol remains not commercially viable. Hamedi and Brinkmann proposed a 1D MR model in Aspen Custom Modeler and apply it for CO_2 hydrogenation to methanol in combination with Aspen Hysys. Their results show a higher improvement for nonadiabatic operation than adiabatic operation compared to the conventional synthesis.[17] The model was also used in an additional work where the influence of the permselectivity of H_2O/H_2 on the overall performance of the methanol synthesis is investigated.[6]

In summary, while similar modeling approaches exist in literature[6,14,17] they typically assume specific membrane properties and investigate the influence of process parameters as well as process design on the overall performance. Within this study, we try instead to close the gap between experimental

work on membrane development and process design. By variation of the membrane permeances and analysis of different MR synthesis loop configurations, we are able to identify performance targets for membrane development. Furthermore, in combining this analysis with an economic assessment we are able to identify cost targets for the membrane that give a good indication for process engineers when membrane reactor application in methanol synthesis is economically viable.

1.3. Separation Mechanisms within Zeolite Membranes

Separation of species across zeolite membranes can be achieved by different kind of mechanisms. In general, transport through inorganic porous membranes are determined by three simultaneous permeation mechanisms: by gaseous diffusion through pores or defects considerably larger than the molecular diameter, by affinity of the permeating species to the membrane material and by mobility or surface diffusion of adsorbed species in the pore network.[13,18] H_2O has a smaller kinetic diameter (0.265 nm) compared to H_2 (0.289 nm), and thus separation can technically be achieved by molecular sieving alone.[17,18] The bigger molecular diameter of methanol (0.390 nm) does not allow for this mechanism. For methanol, adsorption with resulting surface diffusion seems to be the decisive mechanism for separation across the membrane.[18] In this instance, the critical point of methanol at 239.4 °C and 80.8 bar plays an important role for the behavior of methanol as vapor or as gas. Above the critical point, methanol is present as gas and shows little to no adsorption at the membrane walls. Due to surface tension, vapor has the ability to adsorb and condense in small capillaries at partial pressures far away from saturation pressure as a free liquid.[18,19] The critical point of H_2O at 374.1 °C and 221 bar assures the presence of H_2O vapor in the operating range of methanol reactors.[20] These circumstances make the choice of operating conditions crucial in MRs for methanol synthesis. In literature, this effect is observed by a maximum methanol conversion in experimental tests at around 240 °C.[8,20,21] Thus, when diffusion of methanol is modeled, temperature and pressure in the reactor should not exceed 240 °C and 80 bar, respectively. For H_2O and H_2 diffusion, the temperatures and pressures can be higher.

2. Experimental Section

2.1. Process Modeling and Configurations

In order to obtain current benchmark values for a techno economic analysis of methanol synthesis, a process model of a traditional methanol synthesis (TR) was investigated in Aspen Plus. The process setup was then changed to enable operation using a MR membrane reactor. The resulting synthesis loop is depicted in **Figure 2**. It included a sweep gas recycle loop in addition to the feed gas recycle, which is also available in the TR process (see Section A1, Supporting Information). The scale of the plant was set to a $\dot{N}_{CO_2}^{in}$ of 100 kmol h^{-1} for both MR and TR processes and the H_2 inlet was adapted according to the $\dot{N}_{H_2}^{in}/\dot{N}_{CO_2}^{in}$ ratio. In this way a comparison between the

Table 1. Overview of achievable permeances of zeolite membranes.

Reference	T	p	$H_2O:CH_3OH:H_2$	Zeolite	$\mathcal{P}_{H_2O}$	$\mathcal{P}_{CH_3OH}$	$\mathcal{P}_{H_2}$
	[°C]	[bar]	[%]		$[molm^2\,s^{-1}\,Pa^{-1}]$	$[molm^2\,s^{-1}\,Pa^{-1}]$	$[molm^2\,s^{-1}\,Pa^{-1}]$
Sato et al. [11]	130	10	3:26:71	FAU	5.5×10^{-7}	2.1×10^{-7}	1.5×10^{-9}
	130	30	3:26:71		4.5×10^{-7}	1.0×10^{-7}	3.0×10^{-9}
	130	50	3:26:71		4.0×10^{-7}	1.1×10^{-7}	4.0×10^{-9}
	180	10	3:26:71		6.0×10^{-7}	2.0×10^{-7}	2.1×10^{-8}
	180	30	3:26:71		3.4×10^{-7}	1.5×10^{-7}	6.2×10^{-8}
	180	50	3:26:71		2.1×10^{-7}	1.1×10^{-7}	2.1×10^{-8}
	180	10	17.5:17.5:65		5.6×10^{-7}	1.5×10^{-7}	3.8×10^{-9}
	180	30	17.5:17.5:65		9.7×10^{-7}	1.3×10^{-7}	6.6×10^{-9}
	180	50	17.5:17.5:65		2.1×10^{-7}	2.3×10^{-7}	3.7×10^{-9}
Sawamura et al. [9]	150	7	53:14:33	MOR	1.0×10^{-8}	1.0×10^{-10}	9.0×10^{-11}
	200	7	53:14:33		1.5×10^{-8}	1.5×10^{-10}	2.0×10^{-10}
	250	7	53:14:33		2.0×10^{-8}	2.0×10^{-10}	3.0×10^{-10}
	150	1	10:80:10		6.0×10^{-8}	–	–
	200	1	10:80:10		7.1×10^{-8}	–	–
Raso et al. [12]	200	–	Reaction involved	Type A	3.5×10^{-8}	1.0×10^{-9}	4.0×10^{-9}
	220	–	Reaction involved		6.0×10^{-8}	3.0×10^{-9}	5.5×10^{-9}
	240	–	Reaction involved		8.5×10^{-8}	3.0×10^{-9}	5.0×10^{-9}
Seshimo et al. [7]	125	40	10:90:0	LTA	9.0×10^{-7}	2.0×10^{-9}	–
	200	40	10:90:0		9.0×10^{-7}	2.0×10^{-8}	–
	125	40	10:90:0	Si-rich	1.0×10^{-6}	3.0×10^{-10}	–
	200	40	10:90:0	LTA	1.0×10^{-6}	1.0×10^{-9}	–
Rohde et al. [13]	150	5		H-SOD	1.0×10^{-6}	–	1.0×10^{-12}

different operating conditions and process setups can be done. For a $\dot{N}_{H_2}^{in}/\dot{N}_{CO_2}^{in}$ ratio of 3.05 this related to a H_2 inlet stream of ≈20 MW for the lower heating value. While this was far below current state-of-the-art MegaMethanol processes[4] this scale had deliberately been chosen as large scale considering current renewable methanol plants and the lower technology readiness of MRs.

In general, two different routes were conceivable: for high separation and permeation across the membrane, a once-through process of the feed gas might be viable, while the sweep gas was circulated. For moderate separation and permeation, the feed gas recycle cannot be omitted. To achieve high methanol yield in a once-through process, preliminary studies conducted for this work have shown necessary permeances of H_2O and CH_3OH in the order of 1×10^{-5} mol m^2 s^{-1} Pa^{-1}, which was far from currently achievable values[7,9,11] and thus the process was not further considered in this work.

The sweep gas was either recycled at atmospheric pressure (MR ATM) or compressed (MR COMP) to the same pressure as the feed gas. In this case, there was no absolute pressure difference of retentate and permeate side, which favored membrane stability and minimized hydrogen diffusion.[8] Still, partial pressure difference was much smaller compared to an atmospheric sweep. This had a negative effect on permeation. Li et al.[10] performed experiments with vacuum at the permeate side of their supported (Na⁺)-gated water conducting mem-

brane. By using vacuum they found that the sweep gas cycle can be omitted. In this case, no partial pressure of product gases arose at the permeate side, which favored diffusion across the membrane. Still, their experiments were conducted in laboratory scale and the implementation of vacuum on the permeate side for industrial processes needed further investigation. Especially membrane stability for high pressure difference can cause problems because small defects amplify hydrogen diffusion, which can make the use of membranes obsolete.[8,20]

Assuming hydrogen diffusion is not completely avoidable, recycle of the sweep gas led to an inevitable increase of hydrogen in the sweep gas recycle. Hence, hydrogen was selected as sweep gas. For both feed and sweep gas cycle 1 mol% was purged to avoid accumulation of inert species. For the compressed sweep process, H_2 as sweep gas led to a higher H_2 partial pressure on the permeate side and hence diffusion from the permeate side to the retentate side. A fresh sweep gas stream was added according to a specified sweep-to-feed-ratio $\dot{N}^S/\dot{N}^F$ at the reactor inlet. To account for pressure loss in the equipment, like heat exchangers and seperators, the overall pressure drop for both gas streams was assumed as 5%. The reactor was modeled in Python and connected to a USER2 block in Aspen Plus using a Fortran interface. A detailed description of the linkage procedure has been given by Dossow et al.[22]

For energetic comparison between the different cases, the energy efficiency η_{LHV} of the process with regard to the lower
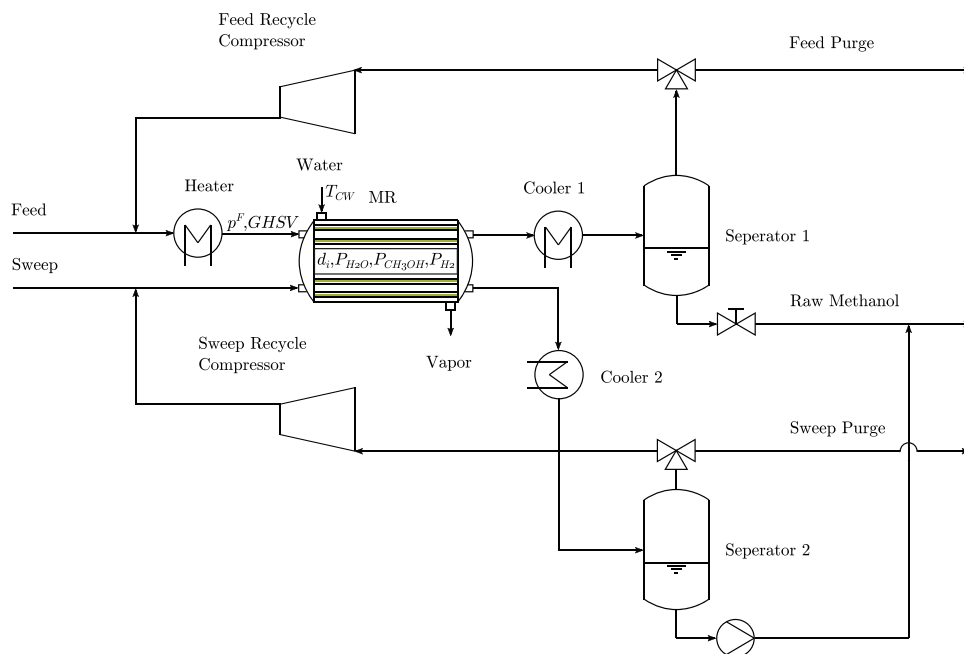
Figure 2. Flowsheet of the atmospheric (MR ATM) and pressurized (MR COMP) membrane methanol synthesis loop.

heating value was used (see Equation 4). For total conversion of CO_2 into methanol in a stoichiometric reaction without considering the compressor power consumption, the resulting efficiency is $\eta_{\text{LVH, stoich}} = 0.8814$.

$$\eta_{\text{LHV}} = \frac{H_{i,\text{CH}_3\text{OH}} \cdot \dot{N}_{\text{CH}_3\text{OH}}^{\text{out}}}{H_{i,\text{H}_2} \cdot \dot{N}_{\text{H}_2}^{\text{in}} + w_{\text{comp,tot}}} \tag{4}$$

2.2. Membrane Reactor Model

A nonadiabatic co-current tube bundle reactor model in Python was used to describe reactions in the feed gas with simultaneous permeation of species across the membrane. The differential equations were solved by the ivp_solve function of the scipy integrate package. The function numerically integrated a system of ordinary differential equations depending on the selected method. An implicit multi-step variable-order (1–5) backward differentiation formula (BDF) method was chosen for the derivative approximation. **Figure 3** illustrates the structure and mathematical model of the reactor. The reactor consisted of multiple steel tubes n_T of diameter d_o with built-in membrane tubes of diameter d_i. For $d_i = 0$ the reactor model operated as a traditional reactor (TR). The membrane as well as the steel tube thickness was not considered in the model instead it was assumed that both were able to fulfill the stability requirements and the respective U_{tube}, U_{mem}, and $\mathcal{P}_j$ values. The reaction took place on the feed (retentate) side. The sweep (permeate) side was used to withdraw permeated species from the reaction zone. The emerging heat during the exothermic reaction was cooled by the sweep gas and an outer cooling fluid. Since heat transfer across inorganic membranes tends to be small,[14,17] most heat had to be removed by the external cooling fluid. For the model boiling water at the desired reactor temperature

was taken as cooling fluid similar to state-of-the art steam raising reactors.

Besides the assumptions of a plug flow reactor, namely: steady state condition, no radial gradients of temperature and concentration, and negligible axial diffusion. Further presumptions were assumed for the reactor behavior: a 1D flow for feed and sweep gas, feed flow at outer side of membrane, and reaction only occurring at catalyst site.

Figure 3 shows a longitudinal cut across one of the reactor tubes with applied differential equation terms. The set of equation (see Equations (5)–(8)) describes the mass and energy balance. The pressure drop across the reaction (fixed bed) and permeation side was calculated by the equation of Ergun (see Equation 9) and Darcy–Weisbach (see Equation 10), respectively. For the friction factor ξ_{pipe} the Colebrook–White equation was used.

$$\frac{\text{d}\dot{N}_j^{\text{F}}(x)}{\text{d}x} = \text{d}\dot{N}_{\text{reac},j} - \text{d}\dot{N}_{\text{diff},j} = \rho_{\text{cat}} \cdot A^{\text{F}} \cdot \sum_k^3 v_{k,j} \cdot r_k - \mathcal{P}_j \cdot \left(p_j^{\text{F}} - p_j^{\text{S}} \right) \cdot \pi \cdot d_i \cdot n_{\text{T}} \tag{5}$$

$$\frac{\text{d}\dot{N}_j^{\text{S}}(x)}{\text{d}x} = \text{d}\dot{N}_{\text{diff},j} = \mathcal{P}_j \cdot \left(p_j^{\text{F}} - p_j^{\text{S}} \right) \cdot \pi \cdot d_i \cdot n_{\text{T}} \tag{6}$$

$$\frac{\text{d}T^{\text{F}}(x)}{\text{d}x} = \frac{\rho_{\text{cat}} \cdot A^{\text{F}} \cdot \sum_k^3 r_k \cdot h_{r,k}}{\dot{N}_{\text{tot}}^{\text{F}} \cdot c_{p,\text{mix}}^{\text{F}}} - \frac{U_{\text{tube}} \cdot \left(T^{\text{F}} - T_{\text{CW}} \right) \cdot \pi \cdot d_o \cdot n_{\text{T}}}{\dot{N}_{\text{tot}}^{\text{F}} \cdot c_{p,\text{mix}}^{\text{F}}} - \frac{U_{\text{mem}} \cdot \left(T^{\text{F}} - T^{\text{S}} \right) \cdot \pi \cdot d_i \cdot n_{\text{T}}}{\dot{N}_{\text{tot}}^{\text{F}} \cdot c_{p,\text{mix}}^{\text{F}}} - \sum_j^{\text{H}_2\text{O,CH}_3\text{OH,H}_2} \text{d}N_{\text{diff},j} \cdot \left(h_j^{\text{F}} - h_j^{\text{S}} \right) \tag{7}$$

$$\frac{\text{d}T^{\text{S}}(x)}{\text{d}x} = -\frac{U_{\text{mem}} \cdot \left(T^{\text{S}} - T^{\text{F}} \right) \cdot \pi \cdot d_i \cdot n_{\text{T}}}{\dot{N}_{\text{tot}}^{\text{S}} \cdot c_{p,\text{mix}}^{\text{S}}} + \sum_j^{\text{H}_2\text{O,CH}_3\text{OH,H}_2} \text{d}N_{\text{diff},j} \cdot \left(h_j^{\text{F}} - h_j^{\text{S}} \right) \tag{8}$$
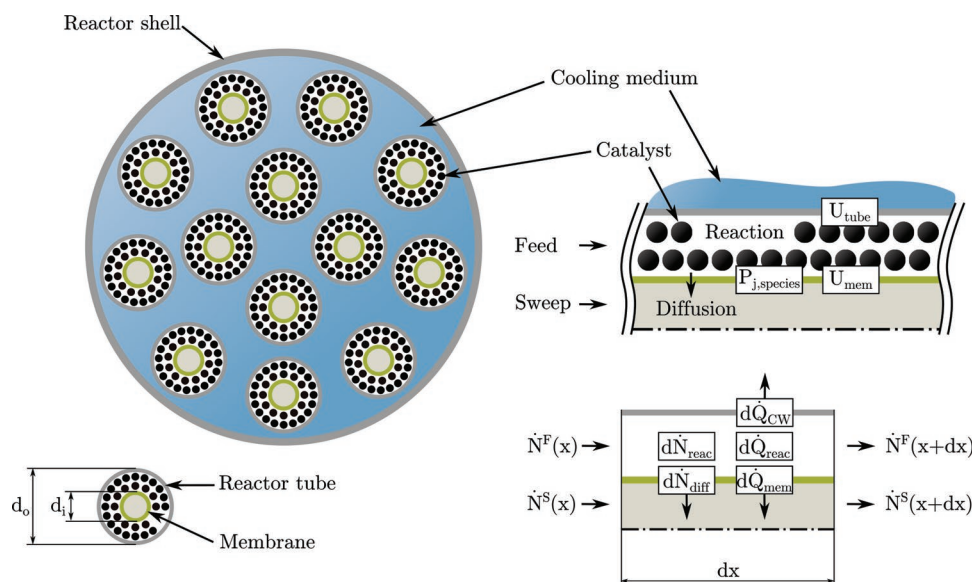
Figure 3. Schematics of MR model.

$$\frac{dp^F(x)}{dx} = -\left(1.75 + 150 \cdot \frac{(1-\varepsilon)}{Re_p}\right) \cdot \frac{(1-\varepsilon)}{\varepsilon^3 \cdot d_p} \cdot \rho_{mix}^F \cdot u_0^{F^2} \quad (9)$$

$$\frac{dp^S(x)}{dx} = \xi_{pipe} \cdot \frac{1}{d_o - d_i} \cdot \rho_{mix}^S \cdot u_0^{S^2} \quad (10)$$

Emerging products of the reactions $d\dot{N}_{reac,j}$ were described by reaction rates r_k taken from literature.[23] A detailed explanation of the implemented reaction kinetic model is given in Section 2.3. Diffusion $d\dot{N}_{diff,j}$ was modeled by a linear function of the species partial pressure difference across the membrane area with the species local permeance $\mathcal{P}_j$ as a constant (see Equation 6). Only diffusion of H_2O, CH_3OH, and H_2 is considered, while CO and CO_2 diffusion was neglected.

As CO_2-hydrogenation was an exothermic reaction, heat was generated in the form of reaction enthalpies $h_{r,k}$. Species transported energy in form of their specific enthalpy h_j across the membrane. Hence, the energy balance took specific enthalpies of crossing species between reaction and permeation zone $h_j^F - h_j^S$ into account. The reaction zone was in thermal contact with the sweep gas side and the cooling water. Corresponding heat transfer coefficients were U_{mem} and U_{tube}, respectively.[14,17] Additional work for correct modeling of heat transfer at reaction condition across zeolite membranes was necessary.

Thermophysical mixture properties of the feed and sweep gas, such as heat capacity $c_{p,mix}$, enthalpy h_j, density ρ_{mix}, molar volume v_{mix}, and viscosity v_{mix} were obtained by the open-source tool Cantera.[24] The areas A^F and A^S, empty tube velocities u_0^F and u_0^S and the Reynolds particle number Re_p were calculated according to Equations (11)–(13) respectively.

$$A^F = \frac{d_o^2 - d_i^2}{4} \cdot \pi$$
$$A^S = \frac{d_i^2}{4} \cdot \pi \quad (11)$$

$$u_0^F = \frac{\dot{N}^F \cdot v_{mix}^F}{A^F}$$
$$u_0^S = \frac{\dot{N}^S \cdot v_{mix}^S}{A^S} \quad (12)$$

$$Re_p = \frac{u_0^F \cdot d_p \cdot \rho_{mix}^F}{v_{mix}^F} \quad (13)$$

In order to get a comprehensive understanding of the behavior of the synthesis loop with and without MR, a total of nine process parameters were investigated, that is, temperature of the cooling agent T_{CW}, pressure of feed p^F, gas hourly space velocity (GHSV), permeances of H_2O, CH_3OH, and H_2 ($\mathcal{P}_j$), the membrane diameter d_i, sweep to feed gas ratio ($\dot{N}^S/\dot{N}^F$), and H_2 to CO_2 ratio of the process inlet streams ($\dot{N}_{H_2}^{in}/\dot{N}_{CO_2}^{in}$). An overview of the value ranges is given in **Table 2**. In order to determine the influence of different model parameters on the processes, they were varied relative to a "base case." The base case parameter are marked bold in Table 2. All constant model parameters are given in Section A2, Supporting Information. The model took a given GHSV as input and calculated the necessary number of tubes n_T as an output parameter. This value was used to obtain investment costs in dependence of the reactor volume. The MR dimensions were oriented on the conventional reactor to allow a direct comparison and focus on the membrane properties and costs. This was only a theoretical assumption and manufacturing of a 10 m long membrane was unlikely to be viable. In reality, similar to commercial reactors for a conventional synthesis, which are not designed as simple tube reactors,[4] a much more rigorous approach would be necessary for the reactor design. The reactor could be splitted in 5 × 2 meter membrane sections. Since the 1D model was not affected by such a design and the focus lies on economic comparison, the reactor length was assumed the same as in the conventional reactor.

GHSV described the volumetric flow rate at standard condition per catalyst volume and is defined in Equation 14.

**ADVANCED
SCIENCE NEWS**

www.advancedsciencenews.com

**ADVANCED
SUSTAINABLE
SYSTEMS**

www.advsustainsys.com

Table 2. Variable and constant model parameters with their respective values, assumptions for the "base case" marked in bold.

Parameter	Unit	Values
Variable parameters		
T_{CW}	°C	220, **230**, 240, 250
p^F	bar	30, 50, **70**
GHSV	h^{-1}	5000, **10 000**, 15 000, 20 000, 25 000
d_i	m	0.02, **0.03**, 0.04, 0.05
$\mathcal{P}_{H_2O}$	mol m^2 s^{-1} Pa^{-1}	0, 1×10^{-8}, 1×10^{-7}, **1×10^{-6}**, 1×10^{-5}
$\mathcal{P}_{CH_3OH}$	mol m^2 s^{-1} Pa^{-1}	0, 1×10^{-8}, **1×10^{-7}**, 1×10^{-6}, 1×10^{-5}
$\mathcal{P}_{H_2}$	mol m^2 s^{-1} Pa^{-1}	1×10^{-10}, **1×10^{-9}**, 1×10^{-8}, 1×10^{-7}
$\mathcal{P}_{CO}$	mol m^2 s^{-1} Pa^{-1}	**0**
$\mathcal{P}_{CO_2}$	mol m^2 s^{-1} Pa^{-1}	**0**
$\dfrac{\dot{N}^{in}_{H_2}}{\dot{N}^{in}_{CO_2}}$	-	2.9, 3, **3.05**, 3.2
$\dfrac{\dot{N}^S}{\dot{N}^F}$	–	0.1, 0.5, **1**, 2, 3

$$GHSV = \frac{\dot{V}^F}{V_{cat}} = \frac{\dot{N}^F \cdot v^0_m}{(1-\varepsilon) \cdot A^F \cdot l \cdot n_T} \tag{14}$$

2.3. Reaction Kinetics

Literature offered numerous kinetic models for methanol synthesis.[23,25–27] Recently, Nestler et al. conducted a critical assessment of existing kinetic rate models for the methanol synthesis and introduced a new kinetic model.[23] Their model considered only direct CO_2-hydrogenation and used fugacities to account for nonideality. Since the model covered a larger range of operating conditions and was validated by numerous experimental data sets, the kinetic model by Nestler et al. was used in this work.

Equation 15 describes the CO_2-hydrogenation and Equation 16 describes the rWGS reaction. Byproduct formation, for example, CH_4 or C_2H_5OH, was not considered because for CO_2-based methanol synthesis usually less than 0.1 wt% of byproducts excluding water is formed.[4] Consequently, their influence on membrane performance for methanol synthesis was neglected.

$$r_1 = \frac{k_1 K_2 f_{CO_2} f_{H_2}^{1.5} \cdot EQ_1}{\left(1 + K_1 f_{CO} + K_2 f_{CO_2}\right)\left(f_{H_2}^{0.5} + K_3 f_{H_2O}\right)} \tag{15}$$

$$r_3 = \frac{k_3 K_2 f_{CO_2} f_{H_2} \cdot EQ_3}{\left(1 + K_1 f_{CO} + K_2 f_{CO_2}\right)\left(f_{H_2}^{0.5} + K_3 f_{H_2O}\right)} \tag{16}$$

Reaction rate constants (k_i & K_i) are given in Section A3, Supporting Information. Mixture fugacity coefficients were calculated by Aspen Plus using the Soave–Redlich–Kwong equation of state (RK-SOAVE) property method. The equilibrium terms EQ_1 and EQ_3 are given in Equations (17) and (18).

$$EQ_1 = 1 - \frac{f_{CH_3OH} f_{H_2O}}{f_{CO_2} f_{H_2}^3 \cdot K_{eq,1}} \tag{17}$$

$$EQ_3 = 1 - \frac{f_{CO} f_{H_2O}}{f_{CO_2} f_{H_2} \cdot K_{eq,3}} \tag{18}$$

The related equilibrium constants were taken from the reassessed chemical equilibria by Graaf et al.[28] (see Equations (19)–(21)). The respective polynomial parameter are given in Section A3, Supporting Information.

$$K_{eq,1} = K_{eq,2} \cdot K_{eq,3} \tag{19}$$

$$\ln K_{eq,2} = \frac{1}{RT} \cdot \left(a_1 + a_2 \cdot T + a_3 \cdot T^2 + a_4 \cdot T^3 + a_5 \cdot T^4 + a_6 \cdot T^5 + a_7 \cdot T \ln T\right) \tag{20}$$

$$\ln K_{eq,3} = \frac{1}{RT} \cdot \left(b_1 + b_2 \cdot T + b_3 \cdot T^2 + b_4 \cdot T^3 + b_5 \cdot T^4 + b_6 \cdot T^5 + b_7 \cdot T \ln T\right) \tag{21}$$

2.4. Economic Assessment

For the economic assessment a simplified approach was chosen based on established cost estimation methods for chemical processes.[29–31] Instead of focusing on a comparison of total production cost for methanol between the conventional and membrane processes, the specific membrane costs c_{mem} were determined according to Equation 22.

$$c_{mem} \leq \frac{\tau_{mem}}{\tau_{plant} \cdot A_{mem}} \cdot \left(\frac{C_{E,TR}}{\eta_{C,MR}} - \frac{C^*_{E,MR}}{\eta_{C,MR}} + C_{Var,TR} - C_{Var,MR}\right) \forall c_{mem} > 0 \tag{22}$$

To offer an economic benefit the membrane costs must be lower or equal to the difference in equipment costs for the conventional process $C_{E, TR}$ and membrane process $C^*_{E,MR}$ and the difference in variable costs of both processes $C_{Var, TR}$ and $C_{Var, TR}$. Assuming the reactor configuration discussed in Section 2.2 the MR costs were approximated as the sum of the equivalently sized conventional reactor and the additional membrane costs. Therefore, $C^*_{E,MP}$ included all process units as well as the equivalently sized conventional reactor without the membrane.

The equipment costs were divided by the respective carbon conversion efficiencies $\eta_{C, TR}$ and $\eta_{C, MR}$ (see Equation 23) to account for differences in the methanol yield. To determine the specific membrane costs c_{mem}, the cost difference was divided by the necessary membrane surface A_{mem} and the number of membrane replacements, which ws given by the ratio of the plant lifetime τ_{plant} to the membrane lifetime τ_{mem}.

$$\eta_C = \frac{\dot{N}^{out}_{CH_3OH}}{\dot{N}^{in}_{CO_2}} \tag{23}$$

For standard equipment cost, correlations from Towler et al.[31] were used. The cost for the conventional methanol reactor were based on van Dijk[32] and scaled with the reactor volume. The year 2020 was selected as the reference year and all cost data was updated using the Chemical Engineering Plant Cost Index (CEPCI)[33] and converted to € using the average annual exchange rate of 2020. All other variable costs were estimated using the factors proposed by Peters et al.[29]. A plant lifetime of 20 years was assumed and operation of 8000 h a^{-1}. A more detailed description of the cost estimation as well as all further boundary conditions is given in Section A4, Supporting Information.

3. Results and Discussion

3.1. Technical Performance of Membrane Processes Compared to Conventional Process

In general, the MR processes show similar behavior compared to the conventional process (TR). Higher pressures result in a more favorable reaction equilibrium conversion consequently improving the methanol yield. The membrane processes reach a maximum methanol yield of (98.9%) at 230 °C cooling temperature, whereas the conventional process achieves highest yields (95.5%) at 240 °C. Energetic efficiency η_{LHV} is roughly 3% higher for both MR base cases compared to the TR base case ($\eta_{LHV}^{TR} = 0.753$). When the recycled sweep is at the same pressure as the feed (MR COMP), higher sweep flow rates are necessary to achieve good permeation. Hence, the total recycle flow rate ($N_{recy}^{F} + N_{recy}^{S}$) of the MR COMP process is 30% higher than the feed recycle flow rate of the traditional reactor ($N_{recy}^{F} = 1560$ kmol h^{-1}). Due to higher partial pressure difference and better permeation the total recycle flow rate of the atmospheric sweep process (MR ATM) is 40% reduced, compared to TR.

Figure 4 shows the energy efficiency (A) as well as the number of tubes within the reactor (B) for varying GHSV and different pressures. For both membrane processes a higher energy efficiency is achieved compared to the TR at equal operating conditions. Higher GHSV lead to shorter residence time of the fluids in the reactor. Hence, conversion is decreased and lower partial pressures of products occur in the feed gas. This leads to reduced diffusion across the membrane, which in turn results in a lower increase in conversion as products are not swept away equally. Consequently, more unreacted gases must be recycled reducing the overall energy efficiency. However, Figure 4 shows that the drop in energy efficiency is still lower for the MR cases with increasing GHSV compared to the TR, in particular at lower pressures. Further the energy efficiency and the methanol yield are directly related and the relationship for different water permeances is shown in Section A.5, Supporting Information.

Increasing the GHSV is equal to reducing the reactor volume or number of reactor tubes for a given feed inlet stream. As a consequence improving the energy efficiency by reducing the GHSV results in a much higher number of tubes within the reactor causing higher investment costs. As can be seen in Figure 4 this effect is not linear due to the complex interplay between the conversion within the reactor, the permeation of the products and the recycle. The TR and MR ATM show a similar decrease in the number of reactor tubes for increasing GHSV (B) while the TR being slightly smaller for the same operating conditions. In contrast, MR COMP sees a steeper decrease in the number of tubes for lower GHSV and approaches the MR ATM for high GHSVs.

With respect to temperatures within the reaction zone, the permeances have a strong influence on heat formation. **Figure 5** shows the hotspot temperature for varying permeances of water and methanol. All other values are kept at the base case conditions. It illustrates the increase in hotspot temperature at the retentate side for improving permeances. This is due to the higher conversion, which emits more reaction heat. This effect is more pronounced for increasing methanol permeances. The reason is that the removal of methanol nearly exclusively benefits the exothermic CO_2- and CO-hydrogenation reactions (see Equations (1) and (2)), while water removal also benefits the endothermic revers water–gas shift reaction (see Equation 3) and has no impact on CO-hydrogenation. Figure 5
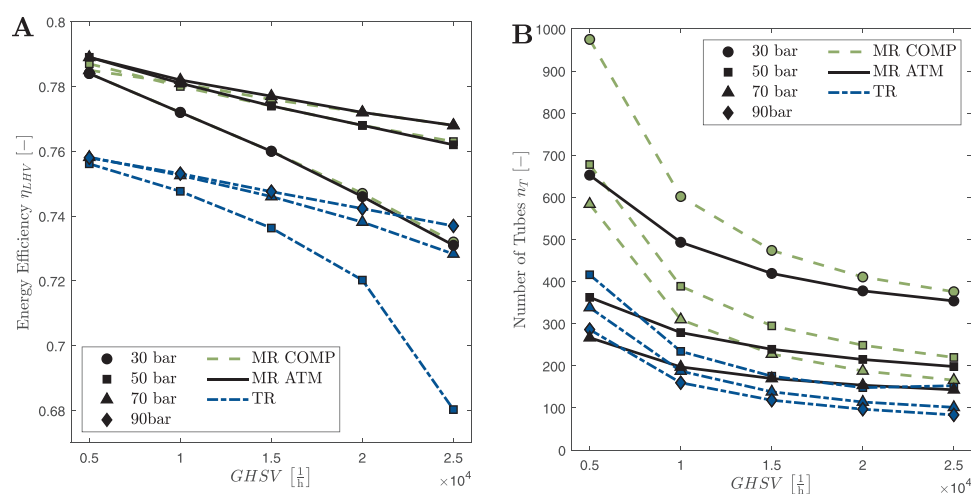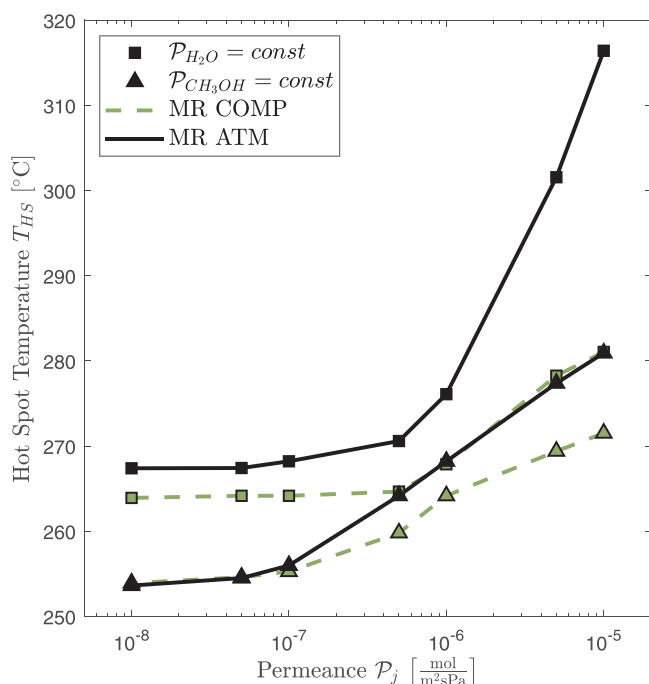

Figure 4. A) Energy efficiency η_{LHV} and B) number of tubes n_T over different GHSV with all other process parameters kept at base case conditions (see Table 2).

Figure 5. Increase in hot spot temperature T_{HS} (maximum temperature within the catalyst bed) in °C over improving permeances of H_2O and CH_3OH with all other process parameters kept at base case conditions (see Table 2).

Figure 6. Methanol yield over different $\mathcal{P}_{H_2}$ with all other process parameters kept at base case conditions (see Table 2).

points out that permeance improvements of the membrane must also be considered in the reactor design in particular with regard to the heat removal. Further, it illustrates the necessity for good thermal stability of the membrane also considering hot catalyst particles in direct contact with the membrane. The effect of local hot spot temperatures above 240 °C on the permeance of methanol needs further investigation, especially under reaction conditions.

MR COMP and MR ATM show different behavior for increasing permeances of H_2. For MR ATM the methanol yield steadily declines with a higher $\mathcal{P}_{H_2}$ (see **Figure 6**). When more of H_2 is permeating from the feed gas to the sweep gas side, the reaction zone is low in H_2 content and the reactions are inhibited. This effect also occurs once the membrane is damaged and small defects are formed. These defects enhance H_2 diffusion until the membrane effect is obsolete. For $\mathcal{P}_{H_2}$ larger than 1×10^{-9} mol m^2 s^{-1} Pa^{-1} the methanol yield sharply drops and process operation becomes unsustainable. Further, the reduction in methanol yield reduces the energy efficiency of the overall process. Therefore, $\mathcal{P}_{H_2}$ is a critical parameter in membrane development for MR ATM processes that must remain below 1×10^{-9} mol m^2 s^{-1} Pa^{-1} during the entire lifetime of the membrane.

Once the sweep gas is compressed to the same pressure as the feed in the MR COMP case, the partial pressure difference of each species between retentate and permeate side is defined by the molar fraction of each species. H_2 as sweep gas means that the partial pressure of H_2 is higher on the permeate side and hence diffusion of H_2 occurs from the permeate side to the retentate side. This circumstance leads to a more stable process
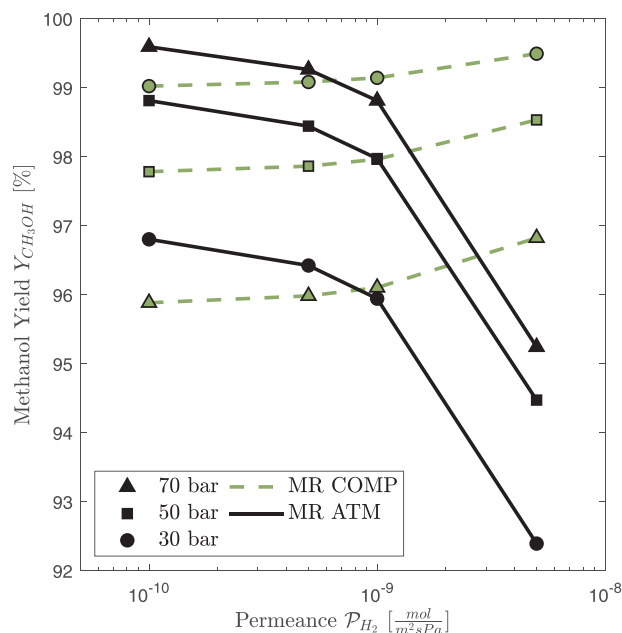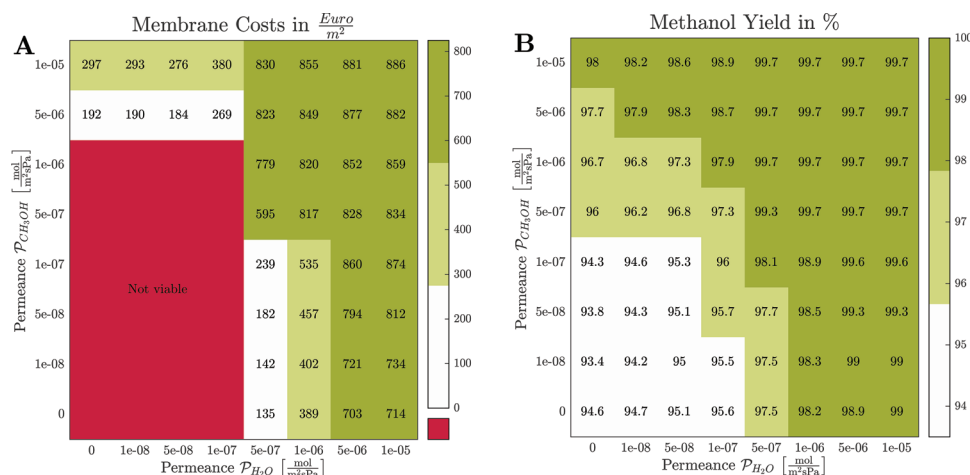
operation if high H_2 permeances occur. The model predicts good methanol yield and η_{LHV} for $\mathcal{P}_{H_2} < 1 \times 10^{-8}$ mol m^2 s^{-1} Pa^{-1}. For higher permeances the H_2 diffusion to the feed gas side gets too high and the rise of feed gas recycle leads to a divergence of the Aspen Plus model.

3.2. Economic Performance of Membrane Reactor Processes

Figure 7 shows the maximum specific membrane costs in the MR ATM case for varying pairs of methanol and water permeances (A) and the respective methanol yields (B) assuming a membrane lifetime of $\tau_{mem} = 2a$. 2 years of membrane lifetime are chosen because this is equal to the catalyst lifetime and would allow the change of catalyst and membrane in the same frequency. Negative specific membrane costs can be viewed as the cases in which the MR ATM process is already more expensive than the TR process without considering the membrane costs. However, because negative membrane costs do not occur in reality, this region is just shown in red as not viable in Figure 7. Hence, for water permeances below 1×10^{-7} mol m^2 s^{-1} Pa^{-1} together with methanol permeances below 1×10^{-6} mol m^2 s^{-1} Pa^{-1} no economic benefit can be achieved. Considering all economic results maximum specific membrane costs should be in the magnitude of 1000 € m^{-2} for a lifetime of 2 years. Typical zeolite membranes costs are estimated around 2000 $ m^{-2}.[34–37] Therefore, this would mean a cost reduction of about 50% with significantly higher requirements regarding thermal and pressure stability as well as lifetime.

Overall the water permeance has a larger influence on the process economics. Consequently, even at very low methanol permeances or no methanol permeation at all, the MR ATM process can offer an economic benefit given sufficiently high

**ADVANCED
SCIENCE NEWS**

www.advancedsciencenews.com

**ADVANCED
SUSTAINABLE
SYSTEMS**

www.advsustainsys.com

Figure 7. A) Maximum specific membrane costs in € m^{-2} and B) methanol yield in % for MR ATM over different $\mathcal{P}_{H_2O}$ and $\mathcal{P}_{CH_3OH}$ for $\tau_{mem} = 2a$ with all other process parameters kept at base case conditions (see Table 2).

water permeances. With regard to the sharp drop in the maximum specific membrane costs for water permeances below 5×10^{-7} mol m^2 s^{-1} Pa^{-1}), this seems like an important target for membrane development and should be achieved over the entire membrane lifetime. Further, 5×10^{-7} mol m^2 s^{-1} Pa^{-1} for both methanol and water permeances is also a critical point for the economic benefit of the MR ATM process because reducing either one of the permeances results in much lower maximum specific membrane costs. As can be seen from Figure 7B this is due to the reduction of the methanol yield below 99%, which results in larger recycle streams and an increased purge of unconverted hydrogen. On the opposite, improving one of the permeances even by an order of magnitude has less effect on the maximum specific membrane costs above this critical point because the methanol yield over the entire process loop already achieves 99% and is mainly limited by the purge gases. In practical terms a more compact reactor design might be achievable for these permeances with reduced reactor length or diameters. Considering the currently more theoretical nature of these very high methanol and water permeances this has not been considered more thoroughly in this work.

Regarding the MR COMP case a similar analysis of the results shows that no economic benefit over the entire range of the investigated permeances is achieved (see Section A3, Supporting Information). This is due to the increased process complexity in comparison to the TR process with the additional compressed sweep recycle. Further, even for large methanol and water permeances the benefit of the MR is limited due to the none existent pressure difference between the retentate and permeate side resulting in small partial pressure differences as driving force of the membrane diffusion.
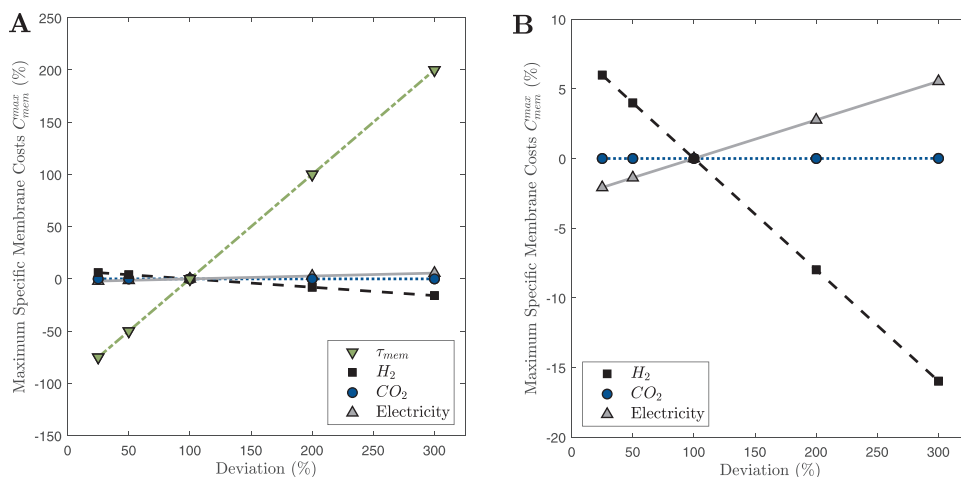
To identify which variables have the highest impact on the maximum specific membrane costs a sensitivity analysis has been conducted. Membrane lifetime, electricity costs, H$_2$ costs and CO$_2$ costs have been varied. **Figure 8**A,B show the results for MR ATM at base case operation. Each variable has been varied one a time from 25% its original value (which is shown as 100% in Figure 8) to 300% while keeping the other values constant. As expected, the membrane lifetime has the

largest impact overall. Increasing the membrane lifetime directly affects how often the membrane must be exchanged over the plants lifetime and is therefore the most important lever to improve the economics of the membrane processes. The CO$_2$ cost have little impact on the total production costs of the methanol in general and also on the economics of the membrane processes. Although costs for CO$_2$ emissions, that is, in the purge gas, have not been considered in this work. Increasing electricity cost improves the economic benefit of the MR ATM case slightly compared to the TR case due to the improved energy efficiency discussed in Section 3.1. The hydrogen cost, however, have the opposite effect due to the additional hydrogen consumption in the sweep cycle of the MR ATM process. Nevertheless, both effects are minor compared to improvements in the membrane lifetime, so for power-to-X processes where the hydrogen costs are directly linked to electricity costs it seems uncertain if higher electricity costs make the MR ATM process more beneficial in this case. Instead it will depend on the efficiency of the realized process plant.

In conclusion, the low impact of variable cost changes on the maximum specific membrane costs suggests that an economic benefit of the MR process is mainly driven by the question if the MR process offers enough advantages in conversion efficiency compared to the difference in investment costs.

4. Conclusion

In this work, the potential for process improvements with MRs has been investigated for the renewable methanol synthesis from H$_2$ and CO$_2$. By coupling a 1D MR Python model with an Aspen Plus simulation of the synthesis loop, a techno-economic assessment was conducted and maximum specific membrane costs were determined. Two cases were considered: A first case where feed and sweep recycle are operated at the same pressure and a second case where the sweep recycle operates at atmospheric pressure. For both cases, advantages in energy efficiency and methanol yield were observed over the entire range of investigated methanol and water permeances.

**ADVANCED
SCIENCE NEWS**
www.advancedsciencenews.com

**ADVANCED
SUSTAINABLE
SYSTEMS**
www.advsustainsys.com

Figure 8. A) Sensitivity analysis of maximum specific membrane cost for MR ATM with variations in membrane lifetime τ_{mem}, B) H_2 costs, CO_2 costs, and electricity costs relative to base case (see Table 2).

Further, in case of the pressurized sweep recycle, hydrogen permeation was not an issue. Nevertheless, the economic evaluation has shown that in this case no economic benefit can be achieved compared to a traditional methanol recycle loop. This is due to the higher process complexity with two recycles, that is, feed and sweep recycle, and a limited membrane performance caused by the equal pressures on the retentate and permeate side.

As a consequence membrane development must focus on material properties that allow an operation with an atmospheric sweep. First and foremost this requires a high pressure stability of the membrane, in particular with regard to the pressure differences of 50–100 bar between retentate and permeate side, which are typical operating pressures for methanol synthesis. Additionally, our results suggest that increasing water and methanol permeances also cause rising hot spot temperatures within the reactor. Therefore, those membrane improvements might cause challenges in reactor design in particular regarding the connection between the membrane and the membrane housing.

Furthermore, a low hydrogen permeance is critical in the case of an atmospheric sweep cycle and should be kept below 1×10^{-9} mol m^2 s^{-1} Pa^{-1} to achieve sufficient methanol yields. The water permeance can be seen as more influential than the methanol permeance. Values larger than 5×10^{-7} mol m^2 s^{-1} Pa^{-1} should be the target. Even membranes with no methanol permeation might offer economic benefits if a sufficiently high water permeance is achieved. Provided that such a highly selective membrane can be manufactured, process configurations might become feasible where no additional methanol purification is necessary. Hence, fuel grade methanol might directly be separated in the feed recycle loop. The technical and economic benefits of such a configuration, however, require further research.

As a starting point for further discussions, and considering the similar characteristics of other renewable fuel synthesis (e.g., methane, dimethyl ether, or Fischer–Tropsch fuels), it is likely that a compressed sweep recycle will always limit the economic benefit of a MR process. Therefore, pressure stability

will play a key role for such membrane reactor applications. However, an atmospheric sweep recycle might be more feasible for other renewable syntheses due to lower operating pressures compared to methanol synthesis (e.g., ≈20 bar for methane synthesis or ≈5 bar for dimethyl ether synthesis). As a consequence, it might be beneficial to target those products first for commercial membrane reactor applications. In addition, it can be expected that membrane developments improving the in-situ removal of products in the reactor will always result in higher hot spot temperatures for exothermic reactions. Therefore, these improvements must always be considered together with thermal stability of the membrane and heat removal within the reactor.

Supporting Information

Supporting Information is available from the Wiley Online Library or from the author.

Acknowledgements

Conflict of Interest

The authors declare no conflict of interest.

Data Availability Statement

The data that support the findings of this study are available from the corresponding author upon reasonable request.

[1] *Power to Fuel*, (Ed: G. Spazzafumo), Elsevier, New York **2021**.

[2] *Ullmann's Encyclopedia of Industrial Chemistry*, (Ed: H. Strathmann), Wiley-VCH, Weinheim **2000**.

[3] *Methanol: The Basic Chemical and Energy Feedstock of the Future*, (Eds: M. Bertau, H. Offermanns, L. Plass, F. Schmidt, H.-J. Wernicke), Springer, Berlin, Heidelberg **2014**.

[4] V. Dieterich, A. Buttler, A. Hanel, H. Spliethoff, S. Fendt, *Energy Environ. Sci.* **2020**, *13*, 3207.

[5] R. P. W. J. Struis, S. Stucki, M. Wiedorn, R. Struis, S. Stucki, M. Wiedorn, *J. Membr. Sci.* **1996**, *113*, 93.

[6] H. Hamedi, T. Brinkmann, S. Shishatskiy, *Membranes* **2021**, *11*, 8.

[7] M. Seshimo, B. Liu, H. R. Lee, K. Yogo, Y. Yamaguchi, N. Shigaki, Y. Mogi, H. Kita, S.-I. Nakao, *Membranes* **2021**, *11*, 7.

[8] J. Gorbe, J. Lasobras, E. Francés, J. Herguido, M. Menéndez, I. Kumakiri, H. Kita, *Sep. Purif. Technol.* **2018**, *200*, 164.

[9] K.-I. Sawamura, T. Shirai, M. Takada, Y. Sekine, E. Kikuchi, M. Matsukata, *Catal. Today* **2008**, *132*, 182.

[10] H. Li, C. Qiu, S. Ren, Q. Dong, S. Zhang, F. Zhou, X. Liang, J. Wang, S. Li, M. Yu, *Science* **2020**, *367*, 667.

[11] K. Sato, K. Sugimoto, Y. Sekine, M. Takada, M. Matsukata, T. Nakane, *Microporous Mesoporous Mater.* **2007**, *101*, 312.

[12] R. Raso, M. Tovar, J. Lasobras, J. Herguido, I. Kumakiri, S. Araki, M. Menéndez, *Catal. Today* **2021**, *364*, 270.

[13] M. Rohde, G. Schaub, S. Khajavi, J. Jansen, F. Kapteijn, *Microporous Mesoporous Mater.* **2008**, *115*, 123.

[14] G. Barbieri, G. Marigliano, G. Golemme, E. Drioli, *Chem. Eng. J.* **2002**, *85*, 53.

[15] F. Galluci, A. Basile, *Int. J. Hydrogen Energy* **2007**, *32*, 5050.

[16] K. Atsonios, K. D. Panopoulos, E. Kakaras, *Int. J. Hydrogen Energy* **2016**, *41*, 792.

[17] H. Hamedi, T. Brinkmann, *ACS Sustainable Chem. Eng.* **2021**, *9*, 7620.

[18] J. Coronas, J. Santamaría, *Sep. Purif. Methods* **1999**, *28*, 127.

[19] M. Matsukata, E. Kikuchi, *Bull. Chem. Soc. Jpn.* **1997**, *70*, 2341.

[20] F. Gallucci, L. Paturzo, A. Basile, *Chem. Eng. Process.: Process Intensif.* **2004**, *43*, 1029.

[21] T. van Tran, N. Le-Phuc, T. H. Nguyen, T. T. Dang, P. T. Ngo, D. A. Nguyen, *Int. J. Chem. React. Eng.* **2018**, *16*, 4.

[22] M. Dossow, V. Dieterich, A. Hanel, H. Spliethoff, S. Fendt, *Renewable Sustainable Energy Rev.* **2021**, *152*, 111670.

[23] F. Nestler, A. R. Schütze, M. Ouda, M. J. Hadrich, A. Schaadt, S. Bajohr, T. Kolb, *Chem .Eng. J.* **2020**, *394*, 124881.

[24] D. G. Goodwin, R. L. Speth, H. K. Moffat, B. W. Weber, Cantera: an object-oriented software toolkit for chemical kinetics, thermodynamics, and transport processes, https://www.cantera.org (accessed: March 2022).

[25] G. H. Graaf, E. J. Stammhuis, A. A. C. M. Beenackers, *Chem. Eng. Sci.* **1988**, *43*, 3185.

[26] K. Bussche, G. F. Froment, *J. Catal.* **1996**, *161*, 1.

[27] Y. Slotboom, M. J. Bos, J. Pieper, V. Vrieswijk, B. Likozar, S. Kersten, D. Brilman, *Chem. Eng. J.* **2020**, *389*, 124181.

[28] G. H. Graaf, J. G. M. Winkelman, *Ind. Eng. Chem. Res.* **2016**, *55*, 5854.

[29] M. S. Peters, K. D. Timmerhaus, R. E. West, *Plant Design and Economics for Chemical Engineers*, 5th ed., McGraw-Hill, Boston **2004**.

[30] R. Turton, R. C. Bailie, W. B. Whiting, J. A. Shaeiwitz, *Analysis, Synthesis and Design of Chemical Processes*, 3rd ed., Prentice Hall, Englewood Cliffs, NJ **2008**.

[31] G. Towler, R. Sinnot, *Chemical Engineering Design*, Butterworth-Heinemann, Oxford **2013**.

[32] K. van Dijk, V. van Eekhout, H. van Hulst, W. Schipper, J. Stam, Methanol from natural gas: final report of the MethRo Collective Design Project **1995**, https://repository.tudelft.nl/islandora/object/uuid%3A8ff7a9c2-4fa6-4701-9aba-f4c38d8c96bf (accessed: March 2022).

[33] Chemical Engineering, the chemical engineering plant cost index, https://www.chemengonline.com/pci-home (accessed: March 2021).

[34] I. G. Wenten, P. T. Dharmawijaya, P. T. P. Aryanti, R. R. Mukti, K. Khoiruddin, *RSC Adv.* **2017**, *7*, 29520.

[35] S. Tennison, *Membr. Technol.* **2000**, *2000*, 4.

[36] G. W. Meindersma, A. B. de Haan, *Desalination* **2002**, *149*, 29.

[37] J. Caro, M. Noack, P. Kölsch, R. Schäfer, *Microporous Mesoporous Mater.* **2000**, *38*, 3.